

# Synthesis of Iron Oxide Nanoparticles by Chemical Co-Precipitation Method and Its Characterization

Aniket Hegade<sup>1</sup>, Ajinkya Bhorde<sup>2</sup>, Ashok Jadhavar<sup>3</sup>, Ravindra Waykar<sup>4</sup>, Subhash Pandharkar<sup>5</sup>, Haribhau Borate<sup>6</sup>, Sagar Nikam<sup>7</sup>, Vikas Mhaske<sup>8</sup>, Sanjay Chakane<sup>\*9</sup>

<sup>1</sup>Department of Physics, Arts, Science & Commerce College, Indapur, Maharashtra, India

<sup>2</sup>Department of Physics, Shri Anand College, Pathardi, Maharashtra, India

<sup>3</sup>Department of Physics, New Arts, Commerce and Science College, Ahmednagar, Maharashtra, India

<sup>4</sup>Department of Physics, Arts, Science and Commerce College, Rahuri, Maharashtra, India

<sup>5</sup>Department of Physics, C.T. Bora College, Shirur, Maharashtra, India

<sup>6</sup>Department of Physics, Annasaheb Waghire College, Otur, Maharashtra, India

<sup>7</sup>Department of Physics, K.R.T. Arts, B.H. Commerce and A.M. Science (KTHM) College, Nashik, Maharashtra, India

<sup>8</sup>Department of Physics, Annasaheb Awate Atrs, Commerce & Hutatma Babu Genu Science College, Manchar, Maharashtra, India

<sup>\*9</sup>Department of Physics, Arts, Science & Commerce College, Indapur, Maharashtra, India

## ABSTRACT

A highly stable and magnetized citric acid (CA)-functionalized iron oxide aqueous colloidal solution ( $\text{Fe}_3\text{O}_4@CA$ ) was synthesized by using a simple and rapid method of one-step co-participation via chemical reaction between ferrous cations in a  $\text{NH}_4\text{OH}$  solution at  $90^\circ\text{C}$ . Followed by CA addition to functionalize the  $\text{Fe}_3\text{O}_4$  surface in 30 min. The nanoparticles (NPs) were synthesized at reported temperatures and shortened time compared with conventional methods. Surface functionalization is highly suggested because bare  $\text{Fe}_3\text{O}_4$  nanoparticles ( $\text{Fe}_3\text{O}_4$  NPs) are frequently deficient due to their low stability and hydrophilicity. Hence, 18-30 nm-sized  $\text{Fe}_3\text{O}_4$  NPs coated with CA ( $\text{Fe}_3\text{O}_4@CA$ ) were synthesized, and their structural, morphological, optical and magnetic properties were characterized using X-ray diffraction, Field emission scanning electron microscope, Fourier transform infrared spectroscopy, and vibrating sample magnetometer. CA successfully modified the  $\text{Fe}_3\text{O}_4$  surface to obtain a stabilized (homogeneous and well dispersed) aqueous colloidal solution. These CA-functionalized NPs with high magnetic saturation (62.49 emu/g) show promising biomedical applications.

**Keywords:** Iron Oxide, Citric acid (CA)-functionalized, co-participation, magnetic saturation, biomedical applications

## I. INTRODUCTION

In present study the research interest in a group of various nano-materials specifically in metal oxides such as magnesium oxide (MgO), copper oxide (CuO), titanium oxide (TiO<sub>2</sub>), iron oxide (Fe<sub>3</sub>O<sub>4</sub>, Fe<sub>2</sub>O<sub>3</sub>) aluminium oxide (Al<sub>2</sub>O<sub>3</sub>), and zinc oxide (ZnO) increases day by day [1-4]. Oxides of metals NPs account for almost one-third of the market for consumer items using nanotechnology and are increasingly being used in a variety of industries [5]. Among these nano-materials a large number of materials have very vast magnetic properties based applications. Because when a magnetic particle's size is lowered below 100 nm, its magnetic characteristics substantially shift. [6-8] These magnetic nano-materials have interesting uses, such as magneto-optical switches, photocatalysis, high density magnetic data storage arrays, electrocatalysis etc. [9-10] Fe<sub>3</sub>O<sub>4</sub> nanoparticles have many advanced application in various fields including magnetic separation, catalytic processes, memory storage devices, magnetic labeling, sensing technologies etc. [11-12] Apart from these uses it is also used in biomedical field to provide contrast effects for magnetic imaging, for the remote control of targeted drug delivery and to induce heating for hyperthermia treatments [13-14]. For the synthesis of Fe<sub>3</sub>O<sub>4</sub> nanoparticles various methods were used such as hydrothermal/solvothermal, co-precipitation, micro-emulsion, electrochemical, and sol-gel [15]. Among these techniques The co-precipitation method is more advantageous than conventional others due to its ease of use and efficiency in the synthesis of Fe<sub>3</sub>O<sub>4</sub> [16]. In the present study we have adopted simple co-precipitation method for the typical synthesis of Fe<sub>3</sub>O<sub>4</sub> nanoparticles. We have studied its structural, optical, morphological and magnetic properties with the help of X-Ray diffraction (XRD), Fourier transform infrared spectroscopy (FTIR), Field emission scanning electron microscopy (FE-SEM) and Vibrating-sample magnetometry (VSM) respectively.

## II. METHODS AND MATERIAL

### A. MATERIALS

All chemicals and reagents were used of analytical grade without any further purification. 0.45 M Ferric chloride (FeCl<sub>3</sub>·6H<sub>2</sub>O), 0.3 M Ferrous sulfate (FeSO<sub>4</sub>·7H<sub>2</sub>O), Ammonium hydroxide 20%, and Citric acid (C<sub>6</sub>H<sub>8</sub>O<sub>7</sub>) were purchased from Loba chemicals. Double-distilled water was used for the synthesis of Fe<sub>3</sub>O<sub>4</sub> solution.

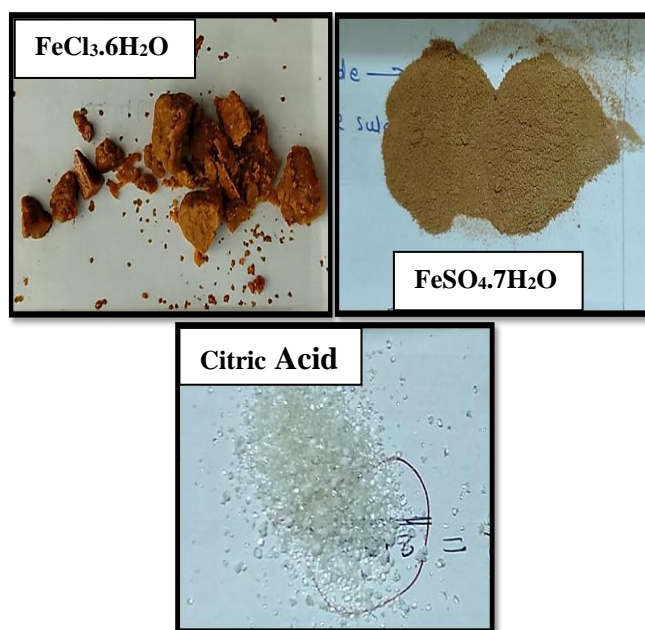
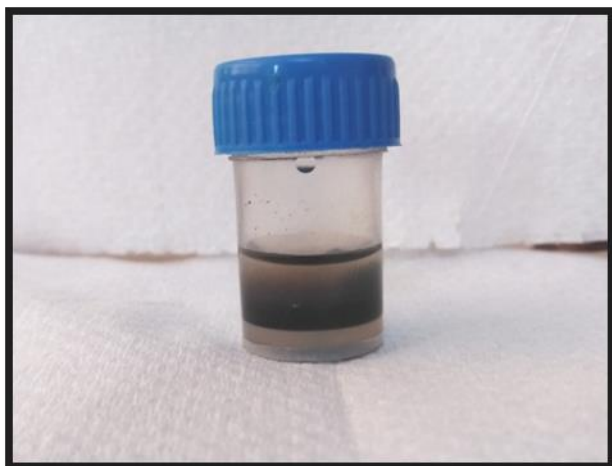


Fig. 1 : Actual photographs of chemical precursors used in the typical synthesis of Fe<sub>3</sub>O<sub>4</sub>.

### B. PREPARATION OF Fe<sub>3</sub>O<sub>4</sub>@CA

The previously reported method was applied for synthesis of bare Fe<sub>3</sub>O<sub>4</sub> magnetic nano-particles and functionalized by Citric acid coating. Briefly, 6.1 g of 0.45 M FeCl<sub>3</sub>·6H<sub>2</sub>O dissolved at 50 mL of distilled water and 4.2 g of 0.3 M FeSO<sub>4</sub>·7H<sub>2</sub>O were dissolved in 50 mL distilled water and heated at 90 °C then afterwards 10 mL of Ammonium hydroxide (25 %) added with constant stirring and 0.5 g of citric acid dissolved in 50 mL of distilled water was added drop wise. The mixture was stirred at 90 °C for 30 min at 650 rpm and then cooled to room temperature. The light brown precipitate was collected and it was

washed with acetone three times to get pure product. After that the precipitate was filtered by using Whitman filter paper no 41. Dried at 60 °C in oven for overnight. Finally Fe<sub>3</sub>O<sub>4</sub> in powdered form obtained using Mortal and Pestle.



**Fig. 2** : Actual photographs of Fe<sub>3</sub>O<sub>4</sub> solution and magnetic attraction of Fe<sub>3</sub>O<sub>4</sub> nano-particles .

### III. RESULTS AND DISCUSSION

#### A. XRD ANALYSIS:

Figure 3 shows the XRD pattern of Iron oxide nanoparticles. The diffraction peaks in the figure confirms the polycrystalline structure of iron oxide nanoparticles. The diffraction pattern gives clear evidence of formation of ferric phase .The diffraction peaks of (220), (311), (400), (422), (511), (440) and (533) reflects the magnetite

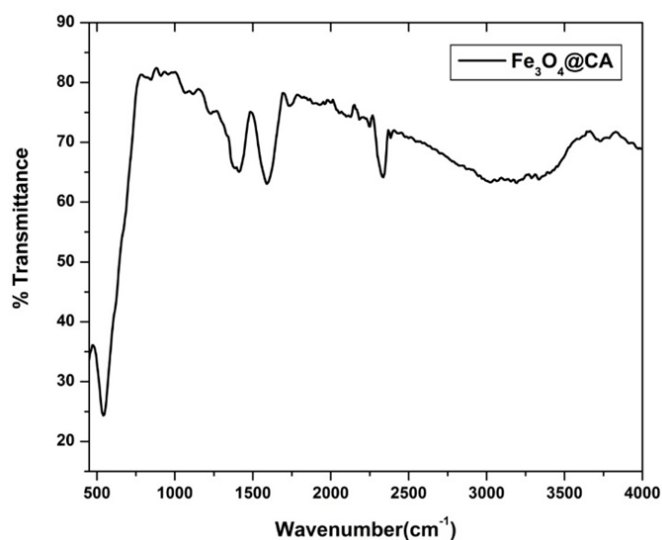


**Fig. 3** : X-Ray diffraction spectra of Fe<sub>3</sub>O<sub>4</sub> nano-particles

crystal with cubic spinel structure [17]. The unit cell of cubic spinel structure consists of eight ferric ions at tetrahedral sites (A sites) each with four oxide ions nearest neighbors, and eight ferric ions and eight ferrous ions at octahedral sites (B sites) each with six oxide ions as the nearest neighbors. This system could be referred to the structural formula of (Fe<sup>3+</sup>)<sub>A</sub>[Fe<sup>2+</sup>Fe<sup>3+</sup>]<sub>B</sub>BO<sub>4</sub> [18]. However, a magnetite can be easily oxidized in air to form the maghemite (Fe<sub>2</sub>O<sub>3</sub>) at temperature 110–230 °C and can be further transformed to the hematite (Fe<sub>2</sub>O<sub>3</sub>) at temperature above 250 °C [19]. Generally, the diffraction peaks at (113), (210), (213) and (210) are the characteristic peaks of maghemite and hematite, respectively [20]. However, these peaks do not appear in the XRD pattern which implies no other iron compounds in the synthesized magnetite.

Comparing the bare magnetite nanoparticles with the coated one, the XRD patterns show similar diffraction peaks; this indicates that the coating agent does not significantly affect the crystal structure of the magnetite nanoparticles [21]. The crystallite size (D) was calculated from X-ray line broadening of the (311) diffraction peak using Debye Scherrer formula [equation (1)].

$$d_{x\text{-ray}} = \frac{0.9 \lambda}{\beta \cos \theta_B} \dots\dots\dots (1)$$

Where  $\beta$  is full-width at half maximum of the strongest intensity diffraction peak (311),  $\lambda$  is wavelength of radiation and  $\theta$  is angle of the strongest characteristic peak. The crystallite size calculated from (311) strongest peak is about 18-20 nm.

**B. FTIR ANALYSIS:**

Successful citric-acid encapsulation of the iron oxide nanoparticles, synthesized using the method as described in the experimental section, was confirmed by the FT-IR result. Fig 4 shows the representative FT-IR spectrum of the citric acid coated particles. The peak at around  $540 \text{ cm}^{-1}$  indicate the presence of an iron oxide skeleton in the sample. The peak near  $1589 \text{ cm}^{-1}$  and  $1411 \text{ cm}^{-1}$ , representing carboxylate ( $\text{COO}^-$ ) stretching, were found in the citric acid coated sample in our experiment. The presence of these peaks is evidence of the formation of the citric acid coating around the iron oxide cores. Moreover, FTIR study confirms the coating of citric acid on the surface of iron oxide nanoparticles.

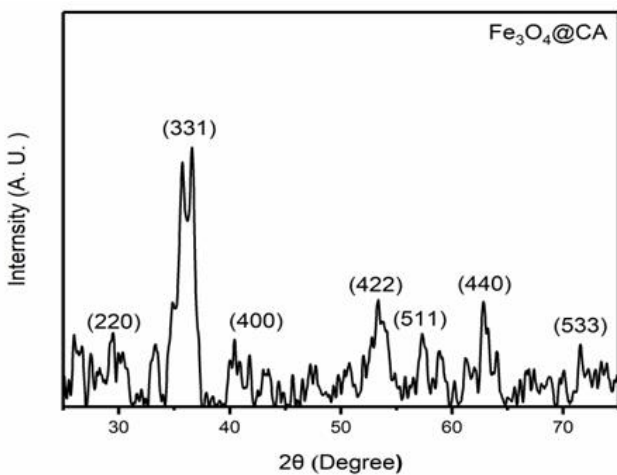


**Fig. 4:** FTIR spectra of Fe<sub>3</sub>O<sub>4</sub> nano-particles.

**C. FE-SEM ANALYSIS:**

Figure 5 shows the FE-SEM images of Iron oxide nanoparticles synthesized by chemical co-precipitation

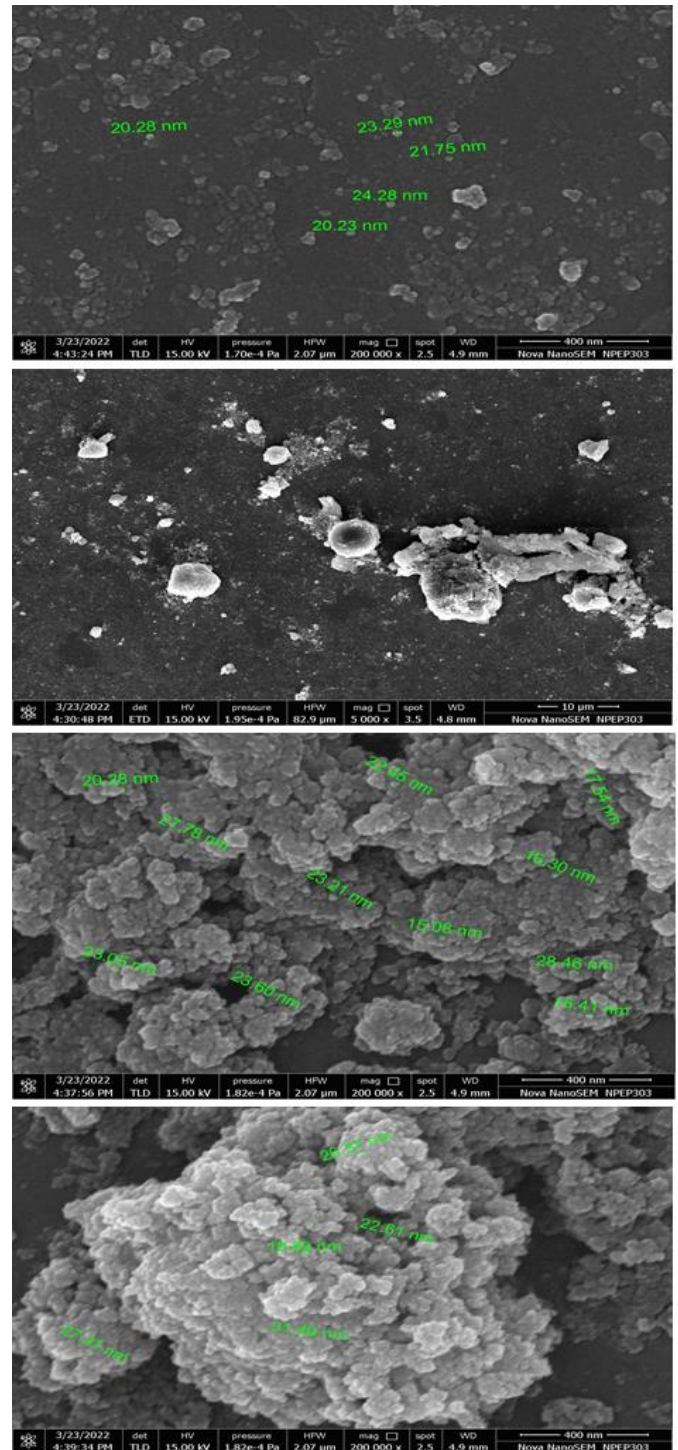


**Fig. 5 :** FE-SEM micrographs of Fe<sub>3</sub>O<sub>4</sub> nano-particles.

method. The surface nanostructural and morphological analysis of iron-NPs using FESEM at

four different magnification are shown in (Fig. 5). The FE-SEM micrograph for the as-prepared sample without surface modification contains small particles that were not uniformly arranged and are highly aggregated [22]. We have depicted the variation in the Iron Oxide nanoparticle sizes using inbuilt FE-SEM software. FESEM images showed predominantly spherical particles about 18-30 nm in diameter (Fig. 7.4).

#### D. VSM ANALYSIS:

The magnetic properties of  $\text{Fe}_3\text{O}_4@CA$  were determined by VSM analysis at 300 °k temperature. The magnetization saturation (emu/g) as a function of the applied magnetic field (Oe) is illustrated in Fig. 6. The magnetization curve shows that the  $\text{Fe}_3\text{O}_4@CA$  NPs exhibit a super paramagnetic behaviour and magnetic saturation ( $M_s$ ) of approximately 62.49 emu/g, which is less than the  $M_s$  for Bulk  $\text{Fe}_3\text{O}_4$  (92 emu/g) and the  $M_s$  for bulk  $\gamma\text{-Fe}_2\text{O}_3$  (744 emu/g) [23]. No hysteresis was observed, and the behaviour was completely reversible at 300 K. Neither coercivity nor remanence was observed. *Arefi et al.* [24] reported that the  $M_s$  of bare  $\text{Fe}_3\text{O}_4$  is reduced after being coated with CA. *Alonso et al.* [25] synthesized  $\text{Fe}_3\text{O}_4$  NPs with high crystallinity of approximately 35 nm and high  $M_s$  of 65 emu/g by using thermal decomposition. The high  $M_s$  value is attributed to the large particle size of  $\text{Fe}_3\text{O}_4$  [26]. Therefore, the  $M_s$  of  $\text{Fe}_3\text{O}_4$  NPs decreases with their reduced particle size due to the increase in surface spin disorder [27, 28]. For biomedical applications such as in hyperthermia and magnetic resonance imaging (MRI), NPs must have a uniform particle size, exhibit super paramagnetism, and possess high  $M_s$ . The as-synthesized  $\text{Fe}_3\text{O}_4@CA$  has a high magnetic response, which is preferable for biomedical applications [24]. Our method shows an advantage of having a simple and rapid route to synthesize highly stable,

monodispersed, and super paramagnetic  $\text{Fe}_3\text{O}_4@CA$  compared with conventional techniques.

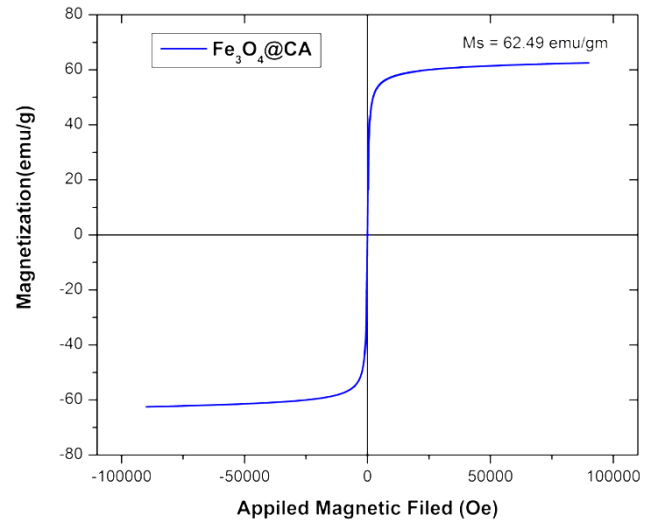


**Fig. 6 :** Magnetization curve of superparamagnetic (no coercivity or remanence)  $\text{Fe}_3\text{O}_4@CA$  at room temperature.

#### IV. CONCLUSION

A highly stable and magnetized citric acid (CA)-functionalized iron oxide aqueous colloidal solution ( $\text{Fe}_3\text{O}_4@CA$ ) was synthesized by using a simple and rapid method of one-step co-participation via chemical reaction between ferrous cations in a  $\text{NH}_4\text{OH}$  solution at 90 °C, followed by CA addition to functionalize the  $\text{Fe}_3\text{O}_4$  surface in 30 min. The NPs were synthesized at reported temperatures and shortened time compared with conventional methods. Surface functionalization is highly suggested because bare  $\text{Fe}_3\text{O}_4$  nanoparticles ( $\text{Fe}_3\text{O}_4$  NPs) are frequently deficient due to their low stability and hydrophilicity. Hence, 18-30 nm-sized  $\text{Fe}_3\text{O}_4$  NPs coated with CA ( $\text{Fe}_3\text{O}_4@CA$ ) were synthesized, and their microstructural, morphological, and magnetic

properties were characterized using X-ray diffraction, Field emission scanning electron microscope, Fourier transform infrared spectroscopy, and vibrating sample magnetometer. CA successfully modified the  $\text{Fe}_3\text{O}_4$  surface to obtain a stabilized (homogeneous and well dispersed) aqueous colloidal solution. These CA-functionalized NPs with high magnetic saturation (62.49 emu/g) show promising biomedical applications.

## V. REFERENCES

- [1] X. Pan, Redding JE, Wiley PA, Wena L, McConnell JS, Zhang B. 2010. Mutagenicity evaluation of metal oxide nanoparticles by the bacterial reverse mutation assay. *Chemosphere* 79:113-116.
- [2] Fahmy, Cormier SA. 2009. Copper oxide nanoparticles induce oxidative stress and cytotoxicity in airway epithelial cells. *Toxicol in Vitro* 23:1365-1371.
- [3] A. Balasubramanyam, N. Sailaja, M. Mahboob, P. Grover 2010. In vitro mutagenicity assessment of aluminium oxide nanomaterials using the Salmonella/microsome assay. *Toxicol in Vitro* 24:1871-1876.
- [4] N. Singh, G. Jenkins, R. Asadib, SH. Doak. 2010. Potential toxicity of superparamagnetic iron oxide nanoparticles (SPION). *Nano Reviews* 1:5358 – DOI: 10.3402/nano.v1i0.5358.
- [5] A. Maynard, R. Aitken, T. Butz, V. Colvin, K. Donaldson, et al. 2006. Safe handling of nanotechnology. *Nature* 444:267-9.
- [6] V. Rotello, Nanoparticles: Building Blocks for Nanotechnology, Ed. Nanostructure Science and Technology Series, (Springer, New York, 2004).
- [7] I. Kelsall, Nanoscale Science and Technology, Ed. by R., Hamley and M. ] Geoghegan, (John Wiley & Sons, Ltd, West Sussex, 2005).
- [8] A. Thiaville and J. Miltat, *Science* 199,2 8 4 ,1939.
- [9] F. E. Kruis, H. Fissan and A. Peled, *J. Aerosol Sci.* 1998, 29, 511.
- [10] T. Thum-Albrecht, J. Schotter, G. A. Kastle, N. Emley, T. Shibauchi, L. Krusin-Elbaum, K. Guarini, C. T. Black, M. T. Tuominen and T. P. Russell, *Science* 2000,290, 2126.
- [11] I. Koh, L. Josephson, *Magnetic Nanoparticle Sensors. Sensors* 2009, 9, 8130–8145
- [12] Y. Chen, A. Kolhatkar, O. Zenasni, *Biosensing Using Magnetic Particle Detection Techniques. Sensors* 2017, 17, 2300.
- [13] M. Colombo, S. Carregal-Romero, M. F. Casula, L. Gutiérrez, *Biological Applications of Magnetic Nanoparticles. Chem. Soc. Rev.* 2012, 41, 4306–4334.
- [14] P. Srinoi, Y. Chen, V. Vittur, M. D. Marquez, T. R. Lee, *Bimetallic Nanoparticles: Enhanced Magnetic and Optical Properties for Emerging Biological Applications. Appl. Sci.* 2018, 8, 1106.
- [15] L. Blaney 2007 Magnetite ( $\text{Fe}_3\text{O}_4$ ): Properties, Synthesis, and Applications *Lehigh Review* 15 33–81.
- [16] K. Petcharoen and A. Sirivat 2012 Synthesis and characterization of magnetite nanoparticles via the chemical co-precipitation method *Mater. Sci. Eng. B* 177 421–427.
- [17] X. Liu, M.D. Kaminski, Y. Guan, H. Chen, H.A.J. Lui, *J. Magn. Mater.* 306 (2006) 248–253
- [18] Samson O. Aisida et al. Biogenic synthesis of iron oxide nanorods using *Moringa oleifera* leaf extract for antibacterial applications. *Applied Nanoscience* July 2019 DOI: 10.1007/s13204-019-01099-x
- [19] T. Yogo, T. Nakamura, W. Sakamoto, S. Hirano, *Journal of Materials Research* 15 (2000) 2114–2120
- [20] J. Murbe, A. Rechtenbach, J. Topfer, *Mater. Chem. Phys.* 110 (2008) 426–433

- [21] Petcharoen, K. and Sirivat, A. (2012) Synthesis and Characterization of Magnetite Nanoparticles via the Chemical Co-Precipitation Method. *Materials Science and Engineering B: Solid-State Materials for Advanced Technology*, 177, 421-427.
- [22] S. O. Aisida et al. Biogenic synthesis of iron oxide nanorods using *Moringa oleifera* leaf extract for antibacterial applications. *Applied Nanoscience* July 2019 DOI: 10.1007/s13204-019-01099-x
- [23] T. Yogo, T. Nakamura, W. Sakamoto, S. Hirano, *Journal of Materials Research* 15 (2000) 2114–2120
- [24] M. Arefi, M. K.Miraki, R. Mostafalu, Citric acid stabilized on the surface of magnetic nanoparticles as an efficient and recyclable catalyst for transamidation of carboxamides, phthalimide, urea and thiourea with amines under neat conditions. *J. Iran. Chem. Soc.* 16, 393–400 (2019).
- [25] Z. Nemati et al. Enhanced magnetic hyperthermia in iron oxide nano-octopods: size and anisotropy effects. *J. Phys. Chem. C* 120, 8370–8379 (2016).
- [26] T. Jayakumar, P. A. Thomas, Protective effect of an extract of the oyster mushroom, *Pleurotus ostreatus*, on antioxidants of major organs of aged rats. *Exp. Gerontol.* 42, 183–191 (2007).
- [27] K. Bakoglidis, K. Simeonidis, D. Sakellari, G. Stefanou, & M. Angelakeris, Size-dependent mechanisms in AC magnetic hyperthermia response of iron-oxide nanoparticles. *IEEE Trans. Magn.* 48, 1320–1323 (2012).
- [28] M.-H. Phan, et al. Exchange bias effects in iron oxide-based nanoparticle systems. *Nanomaterials* 6, 221 (2016).